Symmetry and light coupling to phononic and collective magnetic excitations in $SrCu_2(BO_3)_2$

A. Gozar,[1,2,*] B. S. Dennis,[1] H. Kageyama,[3] and G. Blumberg[1,†]
[1]*Bell Laboratories, Lucent Technologies, Murray Hill, New Jersey 07974, USA*
[2]*University of Illinois at Urbana-Champaign, Urbana, Illinois 61801-3080, USA*
[3]*Department of Chemistry, Graduate School of Science, Kyoto University, Kyoto 606-8502, Japan*
(Received 1 July 2004; revised manuscript received 6 June 2005; published 3 August 2005)

We perform a low temperature Raman scattering study of phononic and collective spin excitations in the orthogonal dimers compound $SrCu_2(BO_3)_2$, focusing on the symmetry and the effects of external fields on the magnetic modes. The zero field symmetry and the behavior in magnetic fields of the elementary and bound magnetic triplet states are experimentally determined. We find that a minimal 4-spin cluster forming the unit cell is able to describe the symmetry as well as the anisotropic dispersions in external fields of the spin gap multiplet branches around 24 cm^{-1}. We identify two Raman coupling mechanisms responsible for the distinct resonance behavior of these magnetic modes and we show that one of these can be ascribed to an effective intradimer Dzyaloshinskii-Moriya spin interaction. Our data also suggest a possible explanation for the existence of a strongly bound two-triplet state in the singlet sector which has an energy below the spin gap. The low temperature phononic spectra suggest strong spin-phonon coupling and show intriguing quasidegeneracy of modes in the context of the present crystal structure determination.

DOI: 10.1103/PhysRevB.72.064405 PACS number(s): 75.10.Jm, 75.50.Ee, 78.30.−j, 71.70.Ej

I. INTRODUCTION

Several properties make $SrCu_2(BO_3)_2$ a unique system among the known quantum magnets. This compound is a realization of a two-dimensional (2D) spin system with a disordered ground state even at very low temperatures and a spin gap $\Delta \approx 24$ cm^{-1} (3 meV) from the singlet ($S=0$) ground state to the lowest excited triplet ($S=1$) state.[1,2] The strengths of the relevant magnetic interactions place this compound close to a quantum critical point (QCP). Moreover, data in high magnetic fields show plateaus at commensurate (1/8, 1/4, and 1/3) values of the saturation magnetization.[2–4] The plateau states can be thought of as crystalline arrangements of magnetic moments separating regions of continuous rise in magnetization, the latter allowing for an interpretation in terms of Bose-Einstein condensation of triplet excitations.[5] It has also been suggested[6] that doping in this system (regarded as a Mott-Hubbard insulator) may lead to a superconducting phase mediated by antiferromagnetic (AF) fluctuations, a mechanism similar in spirit to one of the scenarios proposed for the high-T_c cuprates.[7]

The $S=1/2$ Cu spins are arranged in weakly coupled 2D layers defining the (ab) plane. In each of these sheets they form orthogonal spin-dimer lattices;[8,9] see Fig. 1(a). At $T_c=395$ K the system undergoes a second order phase transition from the space group $I4/mcm$ to $I\bar{4}2m$ on cooling down from the high temperature side. In the $I4/mcm$ phase the planes containing the Cu atoms are flat and they form mirror symmetry elements. The transition at 395 K can be understood as the buckling of the Cu planes which lose their mirror symmetry property. Inversion symmetry is lost as well below T_c but the number of atoms in the unit cell remains unchanged due to the orthogonality of the spin-dimer network. Because of the same orthogonal arrangement, there are two spin dimers in the unit cell. As a result, the spin gap excitation, defined as the transition from the $S=0$ ground state to that (usually the lowest in energy) $S=1$ level whose wave function contains a single spin dimer excited to the triplet state,[1,10,11] has a "fine structure" made out of six levels, three from each dimer in the unit cell.

The 2D spin-dimer lattice can be described well by taking into account the nearest and next nearest neighbor AF superexchange interactions J_1 and J_2, respectively; see Fig. 1(a). In this approximation and for a ratio $x=J_2/J_1$ lower than about 0.7, the direct product of singlet dimers on each rung, which is always an exact eigenstate of the Hamiltonian, is also the ground state of the system and the spin gap is finite although it gets renormalized down with increasing x due to many body effects.[10,12] For large x the ground state changes and the Hamiltonian has long range AF order, other possible

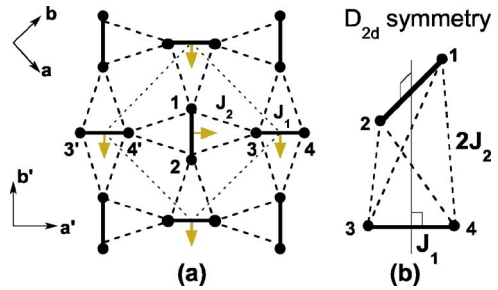

FIG. 1. (Color online) (a) The structure of the spin-dimer compound $SrCu_2(BO_3)_2$. The unit cell is shown by the short dashed square. The circles are the $S=1/2$ Cu spins; the solid and long dashed lines represent the intradimer (J_1) and interdimer (J_2) AF superexchange interactions. The arrows correspond to the proposed intradimer antisymmetric spin interaction d_{ab}. Below 395 K the orthogonal dimers are no longer coplanar. (b) The 4-spin cluster corresponding to the unit cell in (a). As expected, the symmetry of this object is D_{2d}, which is the point group associated with the crystal space group of $SrCu_2(BO_3)_2$ below 395 K. Note that the interdimer superexchange J_2 is effectively doubled if periodic boundary conditions are used.

 ©2005 The American Physical Society

intervening states separated by QCP's being proposed to exist around 0.7; see Ref. 1. Based on fits to magnetization data, predictions of symmetries, relative energies, and dispersions of single and composite triplet excitations, theoretical estimates for x range from 0.603 (Refs. 10 and 11) to about 0.68 (Refs. 12 and 13).

An analysis of the vibrational modes is of interest in $SrCu_2(BO_3)_2$ because spin-lattice interaction has been suggested to be relevant to the magnetic dynamics at low temperatures and high magnetic fields. In particular, spin-phonon interaction has been invoked in order to explain the selection rules of the magnetic transitions seen in infrared (IR) absorption.[15] The coupling between the lattice and magnetic degrees of freedom was also taken into account in order to describe the spin density profile at high fields in the magnetization plateau states.[4] So far the study of phononic excitations has been related mostly to the crystallographic changes at 395 K. It has been established in Refs. 9 and 14 that the structural transition displays soft mode behavior (see Refs. 9 and 14 also for a phononic symmetry analysis). The phononic mode which condenses at 395 K belongs to the B_{1u} representation of the high temperature symmetry group and, in terms of Cu atoms, it involves essentially an alternate displacement along the c axis of the nearest neighbor dimers. Interestingly, several phonons appearing below T_c were observed in (ca) polarization as very close in energy shoulders of some of the modes found above the transition. Due to the absence of inversion symmetry below 395 K this experimental fact suggested the existence of almost degenerate even and odd (transforming like the E_g and E_u representations respectively) excitations in the high temperature phase.[14]

In terms of magnetic properties, elementary and two-triplet excitations have been studied by inelastic neutron scattering (INS),[16,17] electron spin resonance (ESR),[18,19] and IR absorption spectroscopy.[15,20] The low temperature Raman scattering results shown in Ref. 21 are focused on composite magnetic excitations in the $S=0$ channel and are used to extract quantitatively the ratio $x=J_2/J_1$. In our Raman study, the emphasis is however on the elementary and composite collective excitations in the $S=1$ sector, the main results being related to the experimental determination of their symmetries and anisotropic behavior in magnetic fields. We are also able to relate some of these new findings to results of a 4-spin cluster analysis as well as to propose an additional effective spin interaction induced by spin-orbit coupling. It has been established that due to the frustrated nature of the magnetic interactions, the one triplet excitations are local, weakly dispersive in the reciprocal space, while two-particle states are more mobile[16] and have contributions from the whole Brillouin zone.[10,11]

In spite of a lot of experimental and theoretical effort for understanding the magnetic properties there are several open questions. An exact determination of the ratio of the exchange interactions x, which is important due to the proximity to the QCP, is still missing. One interesting aspect in this regard is the observation of a magnetic state at 21.5 cm^{-1}, which is *below* the energy of the spin gap multiplet Δ. This could be seen in ESR,[19] INS,[17] and IR[15] data in energy level anticrossings in the downward dispersions with magnetic field of some of the spin gap branches. The existence of such a low energy mode brings into question the exact quantitative estimation of the AF exchange parameters. As we will show, a direct comparison between our experimental findings and theoretical predictions regarding the symmetry of these modes is illuminating in this respect.

A different set of questions is related to the way the external radiation field couples to the magnetic excitations. While the photon induced spin-exchange process insures the Raman coupling to $S=0$ two-triplet excitations,[21,22] the transitions to $S=1$ states require the presence of spin-orbit coupling.[22] Although an effective antisymmetric Dzyaloshinskii-Moriya (DM) term originating in the spin-orbit interaction [the H_c^{DM} contribution explicitly written in Eq. (3)] has been proposed to explain the "fine structure" of the six levels forming the gap multiplet around 24 cm^{-1} seen in a neutron scattering study, Ref. 17, this term does not mix the singlet ground state to excited $S=1$ states. As a result, the nature of the coupling leading to the observed ESR and IR data is still to be understood. Possible candidates were suggested in the discussion of ESR data[19] and dynamical spin-phonon induced effective DM interactions have been invoked in order to explain the optical absorption spectra.[15,20]

In this article we study phononic modes and collective magnetic excitations in $SrCu_2(BO_3)_2$ with the experimental emphasis placed on the understanding of the magnetic Raman scattering in the $S=1$ channel. In the low temperature in-plane polarized phononic spectra we find (in the 50–350 cm^{-1} energy range) several pairs of modes with similar energies. This quasidegeneracy is intriguing because group theory analysis suggests that they are related to different atomic vibrational patterns. Regarding the magnetic Raman scattering data, our novel findings are the following. The symmetry analysis and exact diagonalization of the 4-spin system Hamiltonian [see Fig. 1(b)] given by

$$H = H_0 + H_c^{DM} + H_{ab}^{DM}, \tag{1}$$

which includes the main, unperturbed, Heisenberg term, H_0, the antisymmetric interdimer DM term proposed in Ref. 17, H_c^{DM}, and an additional intradimer DM term, H_{ab}^{DM}, reading

$$H_0 = J_1 \sum_{(i,j)NN} \mathbf{S}_i \cdot \mathbf{S}_j + J_2 \sum_{(i,j)NNN} \mathbf{S}_i \cdot \mathbf{S}_j, \tag{2}$$

$$H_c^{DM} = \sum_{(i,j)NNN} \vec{d}_c^{(i,j)} (\mathbf{S}_i \times \mathbf{S}_j), \tag{3}$$

$$H_{ab}^{DM} = \sum_{(i,j)NN} \vec{d}_{ab}^{(i,j)} (\mathbf{S}_i \times \mathbf{S}_j) \tag{4}$$

explains the experimentally determined symmetries of the zero field Brillouin zone center spin gap branches around 24 cm^{-1} (confirming the local nature of the elementary one-triplet modes) but fails to account for the two-triplet excitations. In the equations above i and j are nearest neighbor (NN) or next nearest neighbor (NNN) Cu sites and $\vec{d}_c$ and $\vec{d}_{ab}$ are inter and intradimer antisymmetric spin interaction vectors. Remaining confined to the 4-spin cluster we find that by introducing the effective intradimer DM interaction H_{ab}^{DM} we are also able to reproduce the observed selection rules and

intensity variations of the spin gap branches in external magnetic fields. These selection rules also require that the energy of the $S=0$ two-triplet bound state formed from spins confined within a unit cell is *below* Δ (in the 4-spin cluster this is equivalent to $x \geqslant 0.5$ in Fig. 4) suggesting a high binding energy for this two particle excitation. In the last section, we also show results of a resonance study which allows us to identify the action of two different light coupling mechanisms to magnetic excitations.

II. EXPERIMENT

Raman scattering from the *ab* surface of a single crystal of $SrCu_2(BO_3)_2$, grown as described in Ref. 23, was performed using an incident power density less than 1 mW focused to a 100 μm diameter spot. The crystallographic axes orientation was determined by x-ray diffraction. The data in magnetic fields, taken at a sample temperature of about 3 K, was acquired with a continuous flow cryostat inserted in the horizontal bore of a superconducting magnet. We used the $\omega_L=1.92$ and 2.6 eV excitation energies of a Kr^+ laser and a triple-grating spectrometer for the analysis of the scattered light. The data were corrected for the spectral response of the spectrometer and CCD detector.

Polarized Raman scattering can probe Brillouin zone center excitations that belong to different symmetry representations within the space group of the crystal structure. We denote by $(\mathbf{e}_{in}\mathbf{e}_{out})$ a configuration in which the incoming/outgoing photons are polarized along the $\mathbf{e}_{in}/\mathbf{e}_{out}$ directions (see Fig. 1 for axes notations). The (RR) and (RL) notations refer to circular polarizations, $\mathbf{e}_{in}=(\hat{a}-i\hat{b})/\sqrt{2}$, with $\mathbf{e}_{out}=\mathbf{e}_{in}$ for (RR) and $\mathbf{e}_{out}=\mathbf{e}_{in}^*$ for the (RL) geometry. The point group associated to the high temperature phase space group of the $SrCu_2(BO_3)_2$ crystal, $I4/mcm$, is D_{4h}. The point group associated to the $I\bar{4}2m$ space group corresponding to the lower temperature phase is D_{2d}. In D_{2d}, the (RR), (RL), (aa), (ab), $(a'a')$, and $(a'b')$ polarizations probe excitations which belong to the A_1+A_2, B_1+B_2, A_1+B_1, A_2+B_2, A_1+B_2, and A_2+B_1 irreducible representations of D_{2d}.

III. PHONONIC SYMMETRIES

In Fig. 2 we show six low temperature Raman spectra excited with the $\omega_L=1.92$ eV laser energy. The arrows point to the observed modes above 60 cm^{-1} and also shown are their energies and symmetries. Magnetic fields do not affect their energies which indicates the phononic nature of these excitations. The modes below 60 cm^{-1} are not indexed since they will be discussed in the next sections. The excitation at 59 cm^{-1} corresponds to the fully symmetric soft mode of the structural transition at 395 K.[9,14] The corresponding two-phonon excitation in the A_1 channel is seen at 121.8 cm^{-1} and very close to it another sharp mode with B_1 symmetry. Similarly to the data in (ca) polarization in Ref. 14, where below 395 K several new modes appear as shoulders of phonons existing above the transition, we observe several pairs of modes having close energies. For example doublet structures are observed around 155 cm^{-1}, where we see a

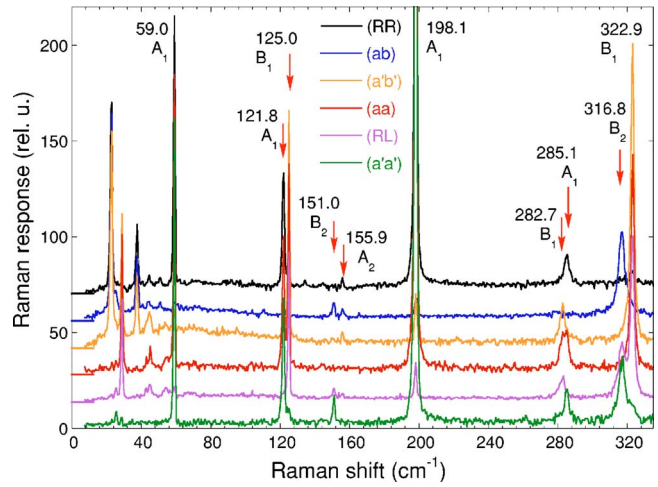

FIG. 2. (Color online) Raman spectra at $T=3$ K in six polarization configurations and zero applied field. Next to each vertical arrow we show the energies (in cm^{-1}) and symmetries of the modes above ≈ 60 cm^{-1}. The spectra are vertically offset. The excitation energy used is $\omega_L=1.92$ eV.

pair of B_2 and A_2 excitations, around 285 cm^{-1}, where we observe two modes having B_1 and A_1 symmetries, and also around 320 cm^{-1} where we see a pair made of B_2 and B_1 symmetric excitations.

One way to explain this behavior, suggested in Ref. 14 is to assume that in the high temperature phase there are phonons which are odd (ungerade: "u") and even (gerade: "g") with respect to inversion but very close in energy and to try to identify them by looking at similar atomic vibrations corresponding to "u" and "g" representations, respectively. Following this idea in more detail and taking into account that the set of irreducible representations $\{A_{1g},A_{2g},B_{1g},B_{2g},A_{1u},A_{2u},B_{1u},B_{2u}\}$ of the D_{4h} point group becomes the set of $\{A_1,A_2,B_1,B_2,B_1,B_2,A_1,A_2\}$ representations (in this order) in D_{2d}, we would have for example that the (A_1,B_1) pair around 284 cm^{-1} corresponds either to a (A_{1g},A_{1u}) group or to a (B_{1u},B_{1g}) group in the high temperature phase. This is because we chose gerade-ungerade pairs and, as shown above, the A_1 symmetric mode can originate either from a A_{1g} or a B_{1u} symmetric phonon while the B_1 mode could be either a B_{1g} or a A_{1u} phonon in the high temperature phase. Similar reasoning would suggest that the (B_1,B_2) group around 320 cm^{-1} originates either from a pair of (B_{1g},A_{2u}) or (B_{2g},A_{1u}) above 395 K and also that the origin of the (B_2,A_2) group around 155 cm^{-1} can be pairs of (B_{2g},B_{2u}) or (A_{2g},B_{1u}) modes in the $I4/mcm$ phase which has D_{4h} as the associated point group.

We performed a symmetry analysis of the $k=0$ atomic vibrations in the high temperature phase and our conclusion is that the approach suggested in Ref. 14 does not provide an *a priori* reason for the quasidegeneracy. This conclusion, as explained in the following, is based just on a simple inspection of the character table of the D_{4h} point group.[24] One can easily note that in D_{4h} the even modes are symmetric with respect to the mirror symmetry in the $Cu(BO_3)$ planes while the odd vibrations are antisymmetric with respect to this symmetry operation. This means that the "u" phonons in the

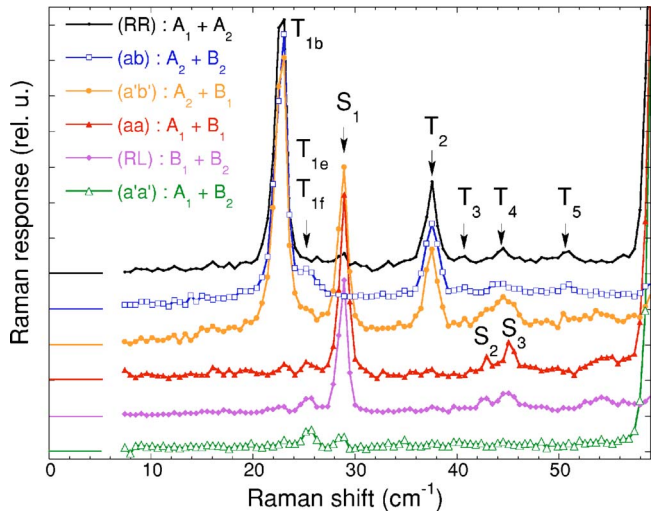

FIG. 3. (Color online) Zero field Raman data taken with the $\omega_L = 1.92$ eV excitation energy at $T = 3$ K in six polarization configurations. The legend shows the tetragonal symmetries probed in each scattering geometry. See the text for notations.

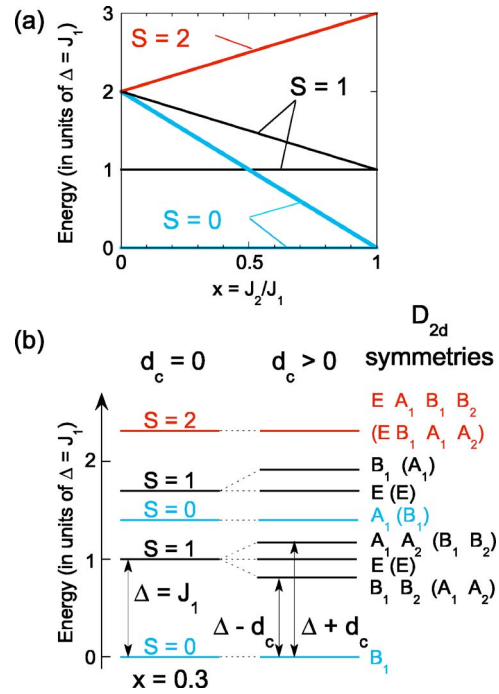

FIG. 4. (Color online) (a) The eigenvalues of the H_0 term of the spin Hamiltonian of Eq. (1) corresponding to the 4-spin cluster shown in Fig. 1(b). The spin gap excitation at $\Delta = J_1$ is six times degenerate in this approximation. (b) Symmetry analysis of the 4-spin cluster in (a) in the D_{2d} group. The energies on the left are calculated for a ratio $x = J_2/J_1$ equal to 0.3. On the right we show the energy splittings and the absolute and relative to the ground state (in parenthesis) symmetries of the 16 magnetic modes when a finite interdimer DM interaction d_c (see Ref. 17) is present. The effect of a finite intradimer DM perturbation, d_{ab}, is to further split the modes which belong to the one-dimensional representations.

high temperature phase correspond to vibrations of the atoms along the c axis while the "g" modes consist of in-plane movements. Due to this difference in the oscillation patterns, one parallel and one perpendicular to the $CuBO_3$ planes, it is hard to explain the closeness of phononic energies at this qualitative level. This is why we find intriguing the observed quasidegeneracy of the phononic modes in the context of the present crystal structure determination.

We remark that on the other hand one could find vibrations which involve similar oscillations at the "molecular" level (for instance groups of atoms forming the Cu-O spin dimer structure or groups of O2 atoms bridging nearest neighbor spin dimers) and which belong to different group representations because of the different "intermolecular" phase pattern. We suggest that, remaining within the conclusions of x-ray studies[9] which so far have not found evidences for additional crystallographic changes at low temperatures (that in turn may produce phonon splittings), good candidates for understanding this behavior are provided by the interdimer BO_3 molecular complexes whose rotations as a whole around the a' and c axes or whose in and out of the plane translations may turn out to be similar in energies. The data suggest that theoretical work in this respect could be interesting.

We note that the appearance of the weak 155.9 cm^{-1} mode in the (RR), (ab), and $(a'b')$ polarizations singles this mode out from the other excitations because it belongs to the A_2 symmetry channel. The Raman coupling to this excitation is unusual compared to the other modes in the sense that it cannot take place *via* two electric dipole transitions. We find several magnetic resonances (see Fig. 3) with A_2 symmetry, but the absence of magnetic field effects suggests that this mode has a preponderant phononic character. A finite intensity of such excitation provides direct evidence for spin-phonon coupling in $SrCu_2(BO_3)_2$.

IV. MAGNETIC SYMMETRIES

The irreducible representations of the D_{2d} point group probed by six scattering geometries, discussed also in the experimental section, are shown in the legend of Fig. 3. In this figure, the six low temperature Raman spectra from Fig. 2 are shown for the frequency region below 60 cm^{-1}. Three strong features around 23, 29, and 38 cm^{-1}, denoted by T_{1b}, S_1, and T_2, are observed and they transform like the A_2, B_1, and A_2 representations respectively. Besides these three modes, we observe several other weaker excitations. Among them we see a set of three A_2 symmetric modes denoted by T_3, T_4, and T_5. We also note the presence of the excitations denoted by T_{1e} and T_{1f} which have B_1 and B_2 symmetries, giving rise to a small feature seen around 25.6 cm^{-1} in all polarizations except for the (RR) configuration. Table I contains a summary of the observed excitations below the 60 cm^{-1} frequency range.

The energies of these Raman active excitations are in agreement with those where INS,[16] ESR,[18,19] and IR[15,20] data observed magnetic modes. The data in magnetic fields (see the discussion in the following section) confirm the magnetic nature and the predominant $S = 1$ character of the "T" modes. Therefore T_{1b}, T_{1e}, and T_{1f} excitations modes seem to belong to the spin gap multiplet while T_2, T_3, T_4, and T_5 would correspond to multiparticle triplet channels.

TABLE I. Collective spin excitations in zero field: notation, the predominant spin character (S_{tot}), the z projection of the spin (S_z), the energies and transition symmetries as observed experimentally and predicted from the 4-spin cluster in Fig. 1 corresponding to $k=0$ excitations. T_{1a} … T_{1f} represent elementary triplet excitations. Generally, the modes whose energies change in external magnetic fields are indexed by T.

Mode	$S_{tot}(S_z)$	Energy	Symmetry Experiment	Symmetry Group theory
T_{1a}	1(±1)	22.8		A_1
T_{1b}	1(±1)	22.8	A_2	A_2
T_{1c}	1 (0)	24.2		E
T_{1d}	1 (0)	24.2		E
T_{1e}	1(±1)	25.6	B_1	B_1
T_{1f}	1(±1)	25.6	B_2	B_2
S_1	0 (0)	28.9	B_1	
T_2	1	37.5	A_2	
T_3	1	40.8	A_2	
S_2	0	43.0	B_1	
T_4	1	44.5	A_2	
S_3	0	45.2	B_1	
T_5	1	50.9	A_2	

If the picture of real space localized elementary triplets is true, then one expects that the analysis of the 4-spin cluster in Fig. 1(b) forming the unit cell is able to predict correctly at least some of the experimentally observed symmetries of these excitations. Besides symmetry analysis, numerical diagonalization of the Hamiltonian of Eq. (1) allows one in principle to also identify the energy as well as the predominant spin character of each eigenstate of this cluster. Indeed, as can be seen by comparing Figs. 3 and 4(b) and looking at the rightmost column of the Table I, the symmetries of the observed zero field one-triplet excitations correspond to the results of group theory analysis. The doubly degenerate E modes, T_{1c} and T_{1d}, are not observed in zero field when the light propagates parallel to the c axis because they are accessible only in (ca) or (cb) polarizations. The observation of the $T_{1e}(T_{1f})$ modes with $B_1(B_2)$ symmetries at an energy of 2.8 cm^{-1} above the A_2 symmetric mode T_{1b} allows the determination of the magnitude of the interdimer interaction d_c [see Fig. 4(b)] and also of its absolute sign.[25] The fully symmetric T_{1a} mode which, within the spin model including only the H_0 and H_c^{DM} terms given in Eqs. (2) and (3), should be degenerate with the strong T_{1b} (A_2 symmetric) excitation at 22.8 cm^{-1} is also not observed which is most probably due to a much weaker coupling to light in this symmetry channel. We will discuss the coupling mechanisms in the last section of our paper.

We turn now to the discussion of two-triplet states. Besides the singlet ground state and six one-triplet states, as can be seen in Fig. 4, the 4-spin cluster analysis predicts the following: one $S=0$ two-triplet bound state in the B_1 channel, three branches with A_1 and doubly degenerate E symmetries which belong to another bound $S=1$ excitation and

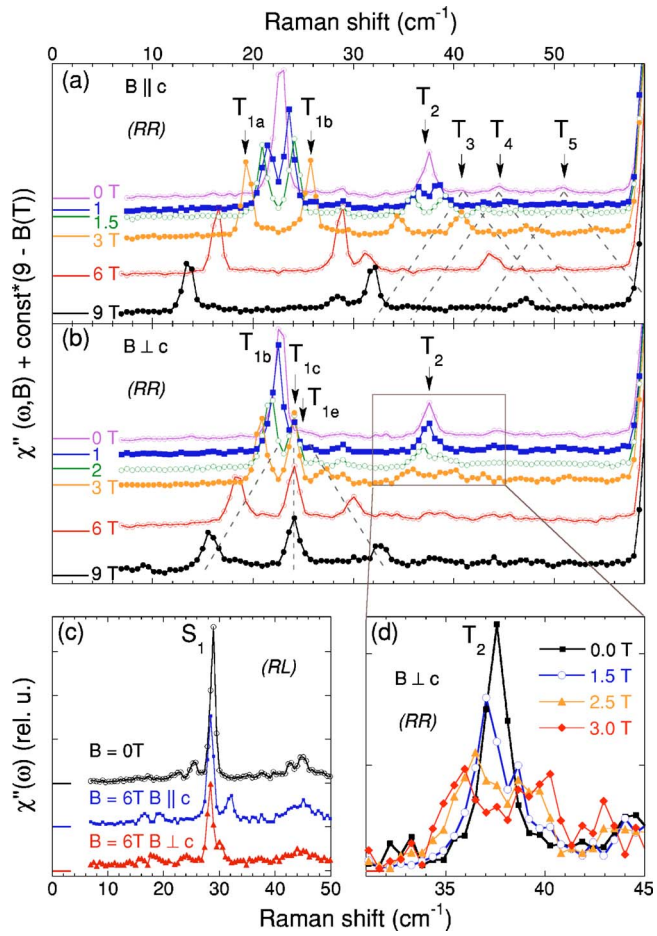

FIG. 5. (Color online) Magnetic field dependencies of the magnetic excitations at $T=3$ K using the $\omega_L=1.92$ eV excitation energy in the following geometries: (a) $(RR)\vec{B}\parallel\hat{c}$; (b) $(RR)\vec{B}\perp\hat{c}$. In (c) the (RL) polarized data is shown for 0 and 6 T magnetic fields for both $\vec{B}\parallel\hat{c}$ and $\vec{B}\perp\hat{c}$. In (a) and (b) the vertical shift is proportional to the magnetic field difference with respect to the 9 T spectrum and the dashed lines are guides for the eye. Panel (d) is a zoomed-in region of panel (b).

five branches of a quintuplet ($S=2$) state having A_1, A_2, B_1, and E symmetries with respect to the ground state. Their energies are plotted in Fig. 4(a) as a function of $x=J_2/J_1$. We note that due to symmetry reasons none of the observed A_2 symmetric modes from T_2 to T_5, having energies higher than 30 cm^{-1}, qualify for an interpretation as triplet bound states generated within the 4-spin cluster. This is consistent with the fact that larger cluster sizes are necessary in order to capture the more delocalized nature of these excitations.

The fact that the existence of the strong A_2 symmetric bound triplet state at an energy $1.55\Delta=37.5$ cm^{-1} has not been predicted by high order perturbative analysis[10] (here we refer especially to the symmetry of this excitation, not its energy) suggests that other spin interactions have to be taken into account in order to explain the excitation spectrum. Apparently the symmetry considerations would allow the 28.9 cm^{-1} feature denoted by S_1 in Fig. 3 to be interpreted as the singlet bound state of two triplets within a unit cell. As we show in the following section, the 28.9 cm^{-1} mode does

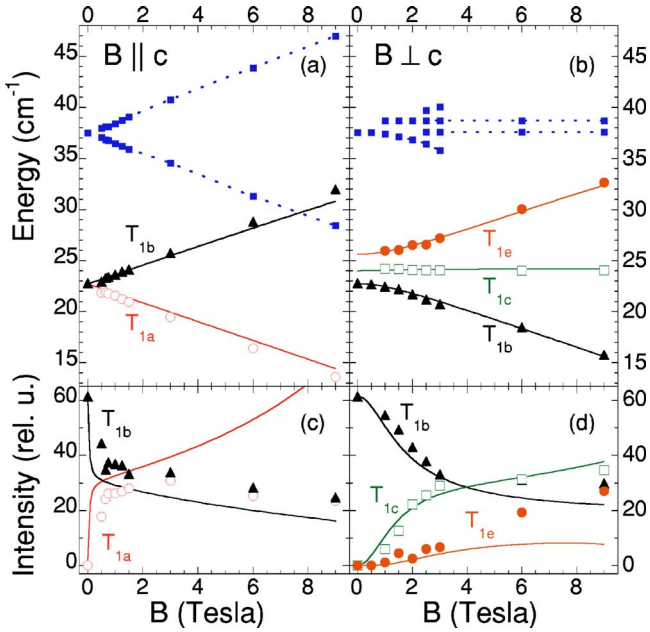

FIG. 6. (Color online) Energies [panels (a) and (b)] and intensities [panels (c) and (d)] of the spin excitations for $\vec{B}\parallel\hat{c}$ (left) and $\vec{B}\perp\hat{c}$ (right) from Figs. 5(a) and 5(b). Symbols represent experimental points, solid lines are the results of 4-spin cluster diagonalization as described in the text, and dashed lines are guides for the eye.

not shift in external fields, which is compatible with a collective singlet excitation as discussed in Ref. 21, but suggests that its internal structure is not the one derived from the 4-spin cluster.

V. MAGNETIC FIELD EFFECTS AT $T\approx 3$ K

In Fig. 5, using the same mode notations, we show the influence of an external magnetic field applied parallel and perpendicular to the c axis on the low temperature Raman spectra from Fig. 3. Here we summarize the relevant aspects, noting first that energy shifts induced by magnetic fields in this figure were observed only for the modes indexed by T in the Table I. In Fig. 5(a) we observe the splitting of the T_{1a} and T_{1b} modes in magnetic fields $\vec{B}\parallel\hat{c}$, the $B=1$ T spectrum showing that the A_2 mode (T_{1b}) present in zero field disperses upwards with increasing magnetic field. Dashed lines mark the dispersion of the much weaker modes T_3, T_4, and T_5. In Fig. 5(b) one of the E modes at 24.2 cm^{-1} becomes Raman active due to symmetry lowering for $\vec{B}\perp\hat{c}$ configuration and we observe three dispersing branches of the gap multiplet. Figure 5(c) shows that the B_1 symmetric excitation at 28.9 cm^{-1} does not change its energy with field, only a very small negative shift of the order of 0.5 cm^{-1} from 0 to 6 T is seen because of the crossing with the upward dispersing gap branches seen in (RR) polarization. Figure 5(d), which is a zoomed-in region of Fig. 5(b), shows that several modes become Raman active in finite fields $\vec{B}\perp\hat{c}$ around 38 cm^{-1} where the T_2 excitation lies. The internal structure of this higher energy multiplet is composed of modes dispersing up, down and independent of magnetic field. We remark on the similarity in selection rules and dynamics in magnetic fields between the collective modes around 38 cm^{-1} and that of the spin gap branches around 24 cm^{-1}. The emergence in finite fields of several strong modes in the spin gap region precludes the observation of the dynamics of the weak T_{1e} and T_{1f} modes from Fig. 3.

Figure 6 summarizes the magnetic field dependencies of the energies and spectral weights of the most intense Raman excitations. The symbols in Figs. 6(a)–6(d) correspond to the experimental data and the solid lines are results of calculations: the energies in panels a and b are obtained by exact diagonalization of the Hamiltonian of Eq. (1) with the parameters specified in the next paragraph; using Fermi's golden rule, the intensities in Fig. 6(c) and 6(d) are calculated as the square of the matrix elements between the ground and excited states of the effective Fleury-Loudon spin interactions describing the coupling to the external electromagnetic field.[22] The form of these interaction terms, denoted by H_1^{int} and H_2^{int}, are discussed explicitly in the next section.

Here we discuss the parameter set used for data fitting in both the $\vec{B}\parallel\hat{c}$ and $\vec{B}\perp\hat{c}$ configurations. Taking into account that (i) the 4-spin cluster neglects many-body gap renormalization effects leading to a singlet-triplet energy independent of $x=J_2/J_1$, see Fig. 4(a), and (ii) the fact that when using periodic boundary conditions there is an effective doubling of the J_2 and interdimer DM interactions, we chose the following values: $J_1=\Delta=24.2$ cm^{-1} which is the value of the spin gap (see the table and Refs. 16–20); $x=0.556$ from the ratio of the energies of the subgap mode at 21.5 cm^{-1}, Refs. 15 and 19, with respect to the gap Δ [see Fig. 4(a)]; an interdimer DM term $d_c=1.4$ cm^{-1}, which produces the splitting of the $T_{1a,b}$ and $T_{1e,f}$ branches from 24.2 cm^{-1} to 22.8 and 25.5 cm^{-1} respectively (our value of d_c is consistent with the one proposed in Ref. 17); finally, using the magnetic field value where the intensities cross in Fig. 6(c), the value of the intradimer interaction was set to $d_{ab}=2.66$ cm^{-1}. We note two aspects regarding the magnitude of the parameters used above. The first is that because many-body spin interactions are not captured within this minimal 4-spin cluster, our chosen value for $x=J_2/J_1$ should not be taken *ad litteram* for the real structure. The second aspect, discussed in more detail later in this section in connection to the dispersion of the magnetic modes in the $\vec{B}\parallel\hat{c}$ configuration, is related to the fact that we were forced to choose $x>0.5$, which is equivalent to saying that the singlet bound state has an energy which is lower than the elementary gap excitation at 24.2 cm^{-1}. This fact may be important regarding the experimental observation of a mode at 21.5 cm^{-1}; see Refs. 15, 17, and 19.

The space group symmetry of the crystal uniquely imposes for any existing static intra-dimer DM interaction [the term H_{ab}^{DM} in Eq. (4)] the configuration depicted in Fig. 1(a), i.e., the DM vectors are perpendicular to the c-axis and dimer bonds. It is the H_{ab}^{DM} term in the system Hamiltonian which is responsible in our interpretation for the mixing of singlet and triplet modes and allows for a finite coupling of the latter excitations to the external photon field. As we mentioned in

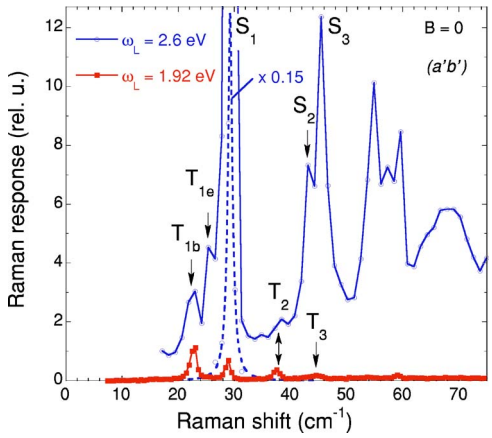

FIG. 7. (Color online) $T=3$ K Raman data in $(a'b')$ polarization for $\omega_L=1.92$ (filled squares) and 2.6 eV (empty circles) excitation energies. The data points corresponding to the resonantly enhanced mode at 29 cm^{-1} are multiplied by 0.15 and the corresponding line represents a Lorentzian fit.

the Introduction, a finite intradimer interaction d_{ab} is crucial because the H_c^{DM} term alone does not mix the singlet and triplet states. Also shown in Fig. 6 by filled squares and dashed lines are the experimental field dependencies of other higher energy modes observed in Fig. 4.

The agreement for this set of parameters is qualitatively good overall and quantitatively better with regard to the energy and intensity variations for the $\vec{B}\perp\hat{c}$ case. As discussed before, the term H_{ab}^{DM} plays a crucial role in obtaining a finite coupling to the excited $S=1$ triplets. H_{ab}^{DM} also produces splittings of the T_{1a} and T_{1b} modes, of the T_{1e} and T_{1f} modes as well as that of the quintuplet branch [these splittings are not shown explicitly in Fig. 4(b)]. For the spin gap branches, the magnitude of the splittings is unresolved because it is very small, of the order of $d_{ab}^2/\Delta\approx 0.25$ cm^{-1}. The largest discrepancy between the experimental data and the calculation is seen in Fig. 6(c). One aspect in this regard is that the value d_{ab} had to be chosen greater than that of d_c. This is unexpected because d_c is allowed by symmetry both above and below the structural phase transition at 395 K while the existence of a finite intradimer DM interaction is allowed only below 395 K, when the mirror symmetry of the (ab) plane is broken. Additional terms may be responsible for this disagreement, possible candidates being the in-plane components of the interdimer DM interaction, which should also be allowed below the structural phase transition.

We now discuss the existence of a magnetic mode *below* the spin gap value.[15,17,19] In order to reproduce the upward dispersion with fields $\vec{B}\parallel\hat{c}$ of the T_{1b} mode we had to choose a value for x which is greater than 0.5, otherwise this excitation would have displayed a downward dispersion. From Fig. 4(a) we observe that $x=J_2/J_1\geqslant 0.5$ implies that the position of the bound singlet state is below Δ. We suggest that precisely this state may be responsible for the observations of the 21.5 cm^{-1} mode in Refs. 15, 17, and 19. The presence of this excitation will also influence specific heat measurements and, in conjunction with the finite intradimer interaction d_{ab}, also the low temperature magnetization data which is not quantitatively understood yet.[1]

The existence of this magnetic mode below the gap seems quantitatively at odds with theoretical predictions.[10,12,13] Nevertheless, perturbational calculations predict the existence of a singlet state at 25 cm^{-1}, which is above but very close to the spin gap.[10] A quantitative reconciliation between theory and the observed selection rules in magnetic fields could be achieved if the coupling ratio $x=J_2/J_1$ is slightly increased from the value of 0.603, as determined in Ref. 10. The experimental finding of the set of A_2 modes (T_2 to T_5 in Fig. 3, all of them below the two-magnon continuum starting at $2\Delta\approx 48$ cm^{-1} and whose symmetries are also not predicted by theory) shows that although several aspects of the magnetic bound states are understood, a complete picture of the spin dynamics in the multitriplet sectors is still to be achieved.

VI. RESONANCE AND LIGHT COUPLING MECHANISMS

Figure 7 shows two low temperature Raman spectra taken in $(a'b')$ polarization with two incoming laser frequencies, $\omega_L=1.92$ and 2.6 eV. The point we want to make in this paragraph is that we observe two qualitatively different behaviors. First we notice that the area under the peak corresponding to the T_{1b} mode in the spectrum taken with the excitation energy $\omega_L=1.92$ is of the same order of magnitude as the one in the spectrum taken with the 2.6 eV laser excitation frequency. The same observation is also true for the mode denoted by T_2. From this perspective, a different behavior is observed for other modes and an example is the group of modes denoted by T_{1e}, S_1, S_2, and S_3. In this latter case for instance, it is clearly seen in our spectra that the mode S_1 in the spectrum taken with the $\omega_L=2.6$ eV excitation is several orders of magnitude stronger than when using the $\omega_L=1.92$ eV laser line. Also, while the modes T_{1e}, S_2, and S_3 are barely visible when $\omega_L=1.92$ eV (see also Fig. 3), they become quite strong for $\omega_L=2.6$ eV. Figure 5 shows in addition that other modes in the 50 to 70 cm^{-1} energy range also become visible only in the $\omega_L=2.6$ eV spectrum. We conclude this paragraph by saying that the group $\{T_{1b},T_2\}$ has a different resonance behavior than the group $\{T_{1e},S_1,S_2,S_3\}$ in the sense that their relative intensities are quite different for the two laser excitation frequencies used.

Note that in the paragraph above we commented only on the *relative* intensities of the Raman modes when the $\omega_L=1.92$ eV excitation was used compared to the 2.6 eV line. Although the absolute intensities of each the Raman excitations can be affected by optical corrections of the data, this effect cancels out when relative intensity ratios are considered. In other words, it is possible in principle that optical corrections can change the ratio of the absolute values of the Raman intensities of the T_{1b} or T_2 modes when taken with $\omega_L=1.92$ and 2.6 eV laser energies, respectively. The same observation applies when we relatively compare the intensities of the T_{1e}, S_1, S_2, and S_3 for these two excitations. However, the important point is that the ratio of intensities should be affected in exactly the same way *if the same resonance mechanism was responsible for both the* $\{T_{1b},T_2\}$ *group of excitations on one hand and for the group of modes* $\{T_{1e},S_1,S_2,S_3\}$ *on the other hand*. The conclusion following

from the above discussion is that the data in Fig. 7 proves the existence of two light coupling mechanisms to the observed low energy excitations. In fact, further support for our statement comes from preliminary data which show that the 1.92 and 2.6 eV laser excitations energies correspond to regions in the visible range where distinct features of the reflectivity spectrum are observed.[26] While certainly interesting in this respect, a complete determination of the optical parameters of $SrCu_2(BO_3)_2$ in the visible range and the identification of the specific high energy electronic intermediate states involved in the coupling mechanisms goes beyond the scope of our article and, as explained above, cannot change our conclusions.

The resonance of the B_1 symmetric T_e magnetic mode, enhanced for $\omega_L=2.6$ eV, is similar to the one corresponding to S_1, S_2, and S_3 excitations as well as to the behavior of the new modes seen around 55, 59, and 68 cm^{-1}. The results of perturbational analysis regarding energy scales and symmetries,[10] in particular of a B_1 symmetric $S=0$ states at 45 cm^{-1}, argues for the magnetic nature of the mode S_3, Ref. 21. Just on the account of the similar resonance behavior of the S_3 excitation with respect to the modes found above 50 cm^{-1} one cannot unambiguously identify the latter as magnetic bound states as well. The lack of energy shift in magnetic fields is consistent with such an interpretation, but the same would be true if they had a phononic origin.

We discuss below the nature of the two light coupling mechanisms to magnetic excitations. For the set of modes discussed in Figs. 6(c) and 6(d) we propose that the coupling takes place *via* the spin-orbit interaction which can be written in an effective form as $H_1^{int} \propto (\mathbf{e}_{in} \times \mathbf{e}_{out}) S_{tot}^z$ (Ref. 22). As it is found experimentally, in zero field this interaction Hamiltonian probes indeed excitations with A_2 symmetry (the T_{1b} mode) and the calculated magnetic field dependent intensities for this and other modes in Figs. 6(c) and 6(d) is also in agreement with the experimental results. The coupling to the T_{1e} and T_{1f} modes from Fig. 3 can be possibly understood if we invoke the usual effective spin interaction corresponding to the photon induced spin exchange process $H_2^{int} \propto \Sigma_{\langle i,j \rangle} (\mathbf{e}_{in} \mathbf{r}_{ij})(\mathbf{e}_{out} \mathbf{r}_{ij}) \mathbf{S}_i \cdot \mathbf{S}_j$. Here the sum runs over pairs of lattice sites, $\mathbf{S}_i$ and $\mathbf{S}_j$ are the exchanged spins on sites i and j, respectively, while $\mathbf{r}_{ij}$ is the vector connecting these sites.[22] The explicit expression of this interaction for several polarizations in the 4-spin cluster approximation contains finite coupling in B_1 and B_2 channels for the triplet T_{1e} and T_{1f} states. This explains the presence of the 25.6 cm^{-1} magnetic modes in all polarizations except (RR).

The difference in the coupling strengths seen in Fig. 7 is thus understandable because these two light coupling mechanisms given by H_1^{int} and H_2^{int} need not be simultaneously in resonance with the same high energy excited electronic states. The photon induced spin exchange Hamiltonian, H_2^{int}, is usually invoked in order to explain Raman active $S=0$ two-magnon type excitations in various magnetic systems.[22] $SrCu_2(BO_3)_2$ is an example where this Hamiltonian, in the presence of singlet-triplet mixing DM interactions, can be used to account for coupling to $S=1$ states. We also note that in principle the photon induced spin exchange could provide coupling to the 21.5 cm^{-1} $S=0$ bound state below the spin gap. The reason this mode is not directly observed in our spectra for any of the two excitation energies used in Fig. 6 is an open question. However, one possible explanation is that the Raman form factor for exciting pairs of $k=0$ magnons is vanishing as opposed to the case zone boundary modes. An example is the case of the Raman vertex calculated for the 2D square lattice within the spin-wave approximation[27] and using the Fleury-Loudon[22] interaction. Consequently, both the 21.5 and the 28.9 cm^{-1} excitations could be attributed to $S=0$ bound states but originating from different parts of the Brillouin zone and having substantially different binding energies.

VII. SUMMARY

We study by Raman scattering collective magnetic excitations in the spin-dimer compound $SrCu_2(BO_3)_2$. Regarding the one-triplet sector, we showed that by using a 4-spin cluster approximation and by including an additional intradimer DM interaction we are able to explain the observed zero field symmetry selection rules and the rich behavior in magnetic fields. We are also able to experimentally demonstrate the existence of two effective magnetic light scattering Hamiltonians which are responsible for their resonance behavior. The 4-spin approximation fails to account for the excitations seen in the multiparticle magnetic sectors. In particular, the existence of a set of four modes below the onset of the two-triplet continuum (at 37.5, 40.8, 44.5, and 50.9 cm^{-1} in the A_2 symmetry channel) shows that further theoretical analysis is required in order to understand the nature of these composite excitations. We suggest a possible explanation for the existence of a subgap collective mode in terms of a strongly bound singlet state which can be generated within the space of 4 nearest neighbor spin dimers.

Experimental data in the energy range below 350 cm^{-1} shows the existence of several quasidegenerate phonons. General symmetry arguments suggest that these excitations, which are very close in energy, involve different vibrational patterns (in plane and c-axis atomic motions, respectively). The failure of group theory to provide an understanding of this interesting behavior at a qualitative level calls for a detailed theoretical investigation of the vibrational modes. We also find a weak A_2 symmetric phonon at 155.9 cm^{-1}. The energy and symmetry of this excitation suggest that this is a coupled spin-phonon excitation and can be evidence for the existence of magnetoelastic interactions in $SrCu_2(BO_3)_2$.

ACKNOWLEDGMENTS

We thank T. Rõõm, G. S. Uhrig, T. Siegrist, and R. Stern for discussions. A.G. also gratefully acknowledges the collaboration with Sasa Dordevic.

*Permanent address: Brookhaven National Laboratory, Upton, NY 11973; Email address: agozar@bnl.gov
†Email address: girsh@bell-labs.com

[1] For a recent theoretical review, see S. Miyahara and K. Ueda, J. Phys.: Condens. Matter **15**, R327 (2003).
[2] H. Kageyama, K. Yoshimura, R. Stern, N. V. Mushnikov, K. Onizuka, M. Kato, K. Kosuge, C. P. Slichter, T. Goto, and Y. Ueda, Phys. Rev. Lett. **82**, 3168 (1999).
[3] K. Onizuka, H. Kageyama, Y. Narumi, K. Kindo, Y. Ueda, and T. Goto, J. Phys. Soc. Jpn. **69**, 1016 (2000).
[4] K. Kodama, M. Takigawa, M. Horvati, C. Berthier, H. Kageyama, Y. Ueda, S. Miyahara, F. Becca, and F. Mila, Science **298**, 395 (2002).
[5] T. M. Rice, Science **298**, 760 (2002).
[6] B. S. Shastry and B. Kumar, Prog. Theor. Phys. Suppl. **145**, 1 (2002).
[7] P. W. Anderson, Science **235**, 1196 (1987).
[8] R. W. Smith and D. A. Keszler, J. Solid State Chem. **93**, 430 (1991).
[9] K. Sparta, G. J. Redhammer, P. Roussel, G. Heger, G. Roth, P. Lemmens, A. Ionescu, M. Grove, G. Güntherodt, F. Hüning, H. Lueken, H. Kageyama, K. Onizuka, and Y. Ueda, Eur. Phys. J. B **19**, 507 (2001).
[10] C. Knetter, A. Bühler, E. Müller-Hartmann, and G. S. Uhrig, Phys. Rev. Lett. **85**, 3958 (2000).
[11] C. Knetter and G. S. Uhrig, Phys. Rev. Lett. **92**, 027204 (2004).
[12] S. Miyahara and K. Ueda, J. Phys. Soc. Jpn. (Suppl.), **69**, 72 (2000).
[13] S. Miyahara and K. Ueda, Phys. Rev. Lett. **82**, 3701 (1999).
[14] K.-Y. Choi, Yu. G. Pashkevich, K. V. Lamonova, H. Kageyama, Y. Ueda, and P. Lemmens, Phys. Rev. B **68**, 104418 (2003).
[15] T. Rõõm, D. Hüvonen, U. Nagel, J. Hwang, T. Timusk, and H. Kageyama, Phys. Rev. B **70**, 144417 (2004).
[16] H. Kageyama, M. Nishi, N. Aso, K. Onizuka, T. Yosihama, K. Nukui, K. Kodama, K. Kakurai, and Y. Ueda, Phys. Rev. Lett. **84**, 5876 (2000).
[17] O. Cépas, K. Kakurai, L. P. Regnault, T. Ziman, J. P. Boucher, N. Aso, M. Nishi, H. Kageyama, and Y. Ueda, Phys. Rev. Lett. **87**, 167205 (2001).
[18] H. Nojiri, H. Kageyama, K. Onizuka, Y. Ueda, and M. Motokawa, J. Phys. Soc. Jpn. **68**, 2906 (1999).
[19] H. Nojiri, H. Kageyama, Y. Ueda, and M. Motokawa, J. Phys. Soc. Jpn. **72**, 3243 (2003).
[20] T. Rõõm, U. Nagel, E. Lippmaa, H. Kageyama, K. Onizuka, and Y. Ueda, Phys. Rev. B **61**, 14342 (2000).
[21] P. Lemmens, M. Grove, M. Fischer, G. Güntherodt, V. N. Kotov, H. Kageyama, K. Onizuka, and Y. Ueda, Phys. Rev. Lett. **85**, 2605 (2000).
[22] P. A. Fleury and R. Loudon, Phys. Rev. **166**, 514 (1968).
[23] H. Kageyama, K. Onizuka, T. Yamauchi, and Y. Ueda, J. Cryst. Growth **206**, 65 (1999).
[24] See, for instance, G. F. Koster, *Properties of the Thirty-Two Point Groups* (M.I.T press, 1963).
[25] A sign change will interchange the position of these modes around the gap at energy Δ.
[26] S. V. Dordevic (private communication).
[27] A. W. Sandvik, S. Capponi, D. Poilblanc, and E. Dagotto, Phys. Rev. B **57**, 8478 (1998).